Unstable Flux Flow due to Heated Electrons in Superconducting Films

Milind N. Kunchur*

Department of Physics and Astronomy, University of South Carolina, Columbia, South Carolina 29208

A flux instability occurs in superconductors at low temperatures, where e-e scattering is more rapid than e-ph, whereby the dissipation significantly elevates the electronic temperature while maintaining a thermal-like distribution function. The reduction in condensate and rise in resistivity produce a nonmonotonic current-voltage response. In contrast to the Larkin-Ovchinnikov instability where the vortex shrinks, in this scenario the vortex expands and the quasiparticle population rises. Measurements in $Y_1Ba_2Cu_3O_{7-\delta}$ agree quantitatively with the distinct predictions of this mechanism.

In a type II superconductor, magnetic fields between the lower critical value H_{c1} and upper critical field H_{c2} introduce flux vortices containing a quantum of flux $\Phi_0 = h/2e$. Here we have superconducting films in a perpendicular applied flux density B, with a transport electric current density j in the plane of the film, which exerts a Lorentz driving force $F_L = j\Phi_0$. The vortex motion generates an electric field $E = vB$ and is opposed by a viscous drag ηv (η is the coefficient of viscosity and v the vortex velocity), so that in steady state $j\Phi_0 = \eta v$ and the response is Ohmic. Larkin and Ovchinnikov (1986) have shown that a dirty superconductor at low temperatures has a free-flux-flow resistivity related to the normal-state value ρ_n by [1]

$$\rho_f/\rho_n \simeq 0.9 B/H_{c2}(T). \qquad (1)$$

Approximately the same result, without the precise 0.9 prefactor, can be obtained by considering the Ohmic dissipation in the core and temporal changes in the order parameter leading to irreversible entropy transfer [2]; the result is also valid for d-wave superconductors that are not superclean [3]. Equation (1) is equivalent to $\eta \approx \Phi_0 H_{c2}/\rho_n$. At low levels of j and E, in the assumed dirty limit $l \ll \xi E_F/kT_c$ (l is the mean free path and E_F is the Fermi energy), η is a constant that is proportional to the order parameter Δ and inversely proportional to the size $\sim \xi^2$ (where ξ is the coherence length) of the vortex. (The Hall effect and transverse component of E are negligible for this discussion, as is vortex pinning because of the large driving forces [4].)

At high electric fields and dissipation levels sufficient to alter the electronic distribution function and/or the electronic temperature, $j(E)$ becomes nonlinear and can develop an unstable region ($dj/dE < 0$) above some critical vortex velocity v^*. For the regime near T_c, such an instability has been predicted by Larkin and Ovchinnikov (LO) [5], and has been experimentally well established [6–9]. At high temperatures, the electron-phonon (e-ph) scattering time $\tau_{e\text{-ph}}$ can be shorter than the electron-electron (e-e) scattering time $\tau_{e\text{-}e}$, preventing internal equilibration of the electronic system and producing a peculiar nonthermal distribution function. Since the order parameter Δ is especially sensitive to the distribution function when close to T_c, even moderate values of E can sufficiently distort Δ (via the Eliashberg mechanism [10]), causing a shrinkage of the vortex core and a removal of quasiparticles from its vicinity. This is the gist of the LO behavior [5,6]. As LO themselves emphasize, the effect is most favorable close to T_c for superconductors with a full gap and, as shown by Bezuglyj and Shklovskij [11], is dominant for $B < B_T$ (with $B_T \sim 0.1$ T for our low-T regime). One of the predictions of the standard LO effect is a v^* that is B independent. This has been confirmed in $Y_1Ba_2Cu_3O_{7-\delta}$ in the high-T range [8,9].

This work investigates the opposite regime of $T \ll T_c$ and $B > B_T$, where Δ is not sensitive to small changes in the distribution function. Furthermore, because $\tau_{e\text{-}e} < \tau_{e\text{-ph}}$ as $T \to 0$, the distribution function remains thermal-like and the electronic system suffers mainly a temperature shift with respect to the lattice [5,11–13]. Then, instead of the standard LO picture described earlier, we consider a more transparent scenario where the main effect of the dissipation is to raise the electronic temperature, create additional quasiparticles, and diminish Δ. The vortex expands rather than shrinks, and the viscous drag is reduced because of a softening of gradients of the vortex profile rather than a removal of quasiparticles. This sequence of events is almost opposite to the standard LO picture and represents a new type of unstable regime prevalent at $T \ll T_c$. All experimental measurables can be calculated without ambiguity, and the predicted field dependencies and full $j(E)$ curves fit the experimental results without any adjustable parameters.

Previously, some deviations from LO behavior at intermediate temperatures—such as a B-dependent v^*—were treated through modifications to the LO effect, such as an intervortex spacing l_ϕ that exceeds the energy-relaxation length l_ϵ [14] or by inclusion of thermal effects [11,12]. Those treatments do not apply to the present $T \ll T_c$ regime where $l_\epsilon \sim \sqrt{D\tau_{e\text{-ph}}} \sim 100$–$1000$ nm is larger than

$l_\phi = 1.075\sqrt{\Phi_0/B} \sim 10$–$50$ nm ($D = 3 \times 10^{-4}$ m^2/s is the diffusion constant [8]).

Here we take a "bottom-up" approach and start from the $T \sim 0$ limit: The total input power jE travels from electrons to lattice and from there to the bath, so that $T_0 < T_p < T'$, where T_0 and T_p are the bath and phonon temperatures, and T' is the raised nonequilibrium electronic temperature. Macroscopic heating, represented by $T_p - T_0 = R_{th}jE$, is $<5\%$ of the total increase $T' - T_0$ for the worst case dissipation so that $T_p \approx T_0$. (Here $R_{th} \sim 1$ nK $\cdot$ cm^3/W is the total thermal resistance between the film and the bath; see experimental section. It will be seen later that the specific-heat integral heavily weights the higher temperatures, so that $T_p - T_0$ is quite negligible.) The energy relaxation between electrons and lattice occurs by inelastic e-ph scattering and is characterized by an effective time $\tau_\epsilon \sim \langle\tau_{e\text{-ph}}\rangle$. The principle contributions to ρ_n come from impurities and phonons. Since the phonon temperature remains near the bath, ρ_n's value will not change as the nonequilibrium T' rises. Thus, putting $\rho_n(T_0)$ and $H_{c2}(T')$ (since H_{c2} does depend on T') into the previous equations gives the $j(E)$ response in terms of T':

$$j = v\eta(T')/\Phi_0 = EH_{c2}(T')/\rho_n(T_0)B. \quad (2)$$

One now has the ingredients for calculating the critical field dependencies in a few steps. The $j(E)$ function of Eq. (2) is nonmonotonic since E is multiplied by $H_{c2}(T')$ [or $\eta(T')$] which drops rapidly to zero as $T' \to T_c$ with increasing dissipation. The instability occurs at $dj/dE = 0$, which happens at a certain value $T' = T^*$ where $H_{c2}(T')$ [or $\eta(T')$] drops sufficiently rapidly. T' depends explicitly only on the power density $jE = \eta v^2 B/\Phi_0$ and on quantities that depend on T' itself (τ_ϵ, specific-heat, etc.). Hence, at the instability, $j^*E^* = v^{*2}\eta(T^*)B/\Phi_0 = $ const, which gives the critical-parameter field dependencies:

$$v^* \propto 1/\sqrt{B}, \quad\quad E^* \propto \sqrt{B}, \\ j^* \propto 1/\sqrt{B}, \quad\quad \text{and} \quad \rho^* \propto B, \quad (3)$$

using $E^* = v^*B$, $j^* = v^*\eta(T^*)/\Phi_0$, and $\rho^* = E^*/j^*$. This gives $v^* \propto 1/\sqrt{B}$ in a natural way, consistent with our measurements in this regime and in contrast to the B-independent v^* of the pure LO effect near T_c.

To derive the complete $j(E)$ response and absolute values of critical parameters, we calculate T' and insert it into Eq. (2). We take $H_{c2}(0) = 120$ T [15] with the Werthamer-Helfand-Hohenberg (WHH) function [16] for interpolation between this $H_{c2}(0) = 120$ and $H_{c2}(T_c) = 0$. [There is some theoretical controversy regarding the exact form of $H_{c2}(T)$; however, empirically, direct measurements [15] of $H_{c2}(T)$, within their uncertainty, seem not to depart drastically from the WHH function, and the exact functional shape does not crucially affect our conclusions.] The dissipation raises the electronic energy by $jE\tau_\epsilon$, which is related to T' by

$$jE\tau_\epsilon \approx \frac{E^2 H_{c2}(T')\tau_\epsilon}{\rho_n(T_0)B} \approx \int_{T_p}^{T'} c(T)dT \approx \int_{T_0}^{T'} c(T)dT, \quad (4)$$

where $c(T)$ is the electronic specific heat. To calculate $c(T)$, Y$_1$Ba$_2$Cu$_3$O$_{7-\delta}$ is modeled as a layered d-wave superconductor: $\Delta_{\vec{k}}(T) = \Delta_0(T)[k_x^2 - k_y^2]/k^2 \approx \Delta_0(T)\cos(2\theta)$, taking the BCS temperature dependence for $\Delta_0(T)$ and $\Delta_0(0) = 19$ meV from tunneling and infrared measurements [17]. Then $c(T) = \partial\{\sum_k E_k f_k\}/\partial T$, where $f_k = [\exp(E_k/k_BT) + 1]^{-1}$ is the Fermi-Dirac distribution, $E_k = \sqrt{\zeta_k^2 + \Delta_k^2}$, $\zeta_k = \epsilon_k - \mu$, and $\mu = 0.2$ eV is the chemical potential [18]. With the replacement of $\sum_k$ by $\int d\zeta N(0)\int d\theta/2\pi$ [where $N(0)$ is the normal density of states at μ], this $c(T)$ is now inserted into Eq. (4), which is integrated numerically to obtain T' and thence $j(E)$ from Eq. (2).

The numerical results of the above calculation are shown in Fig. 1. The $j(E)$ curves of panel (a) have an infinite slope at the instability (j^*, E^*), indicated by arrows, and then exhibit negative slope. This negative-sloped portion is experimentally forbidden in a current-biased measurement and instead will be manifested as a vertical jump in E. The electronic temperature T' rises from the bath value T_0 to T^* at the instability. Panel (b) shows the computed T^*, which is independent of B as expected but has a slight dependence on the bath temperature T_0.

In order to conveniently scale the experimental curves, the exact numerical $j(E)$ function derived above—and plotted in Fig. 1—can be cast into a mathematically more manageable form by noting that the right-hand side of Eq. (4) [which represents the internal-energy difference $U(T') - U(T_p)$] can be approximated by $jE\tau_\epsilon \approx \Delta(T')n_q(T') - \Delta(T_p)n_q(T_p) \approx \Delta(T')n_q(T')$ [since $U(T)$ is a rapidly increasing function]. Δ and n_q are connected through the statistical equations of the previous paragraph. By taking the anisotropic d-wave gap together with a BCS temperature dependence as discussed above,
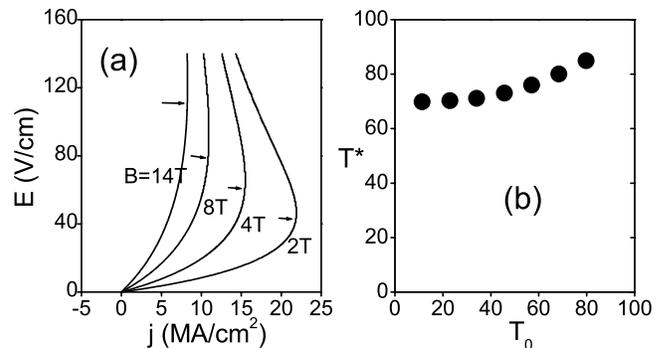

FIG. 1. Numerical results obtained from solving Eq. (4), as described in the text. (a) Theoretical $j(E)$ curves at $T_0 = 0$ K. The onset of negative slope, indicated by arrows, marks the instabilities. (b) The critical temperature T^* for different initial temperatures T_0; T^* is independent of B and τ_ϵ.

the number of quasiparticles excited above the gap were numerically computed to obtain the following d-wave generalization of the $\Delta - n_q$ relationship: $(\Delta/\Delta_0)^2 = f(n_q/n)$, where $n = 2.7 \times 10^{21}$ cm^{-3} is the carrier concentration and $f(x) \simeq 1 - 0.4386x - 1539x^2 + 40\,381x^3 - 345\,217x^4$ [despite the appearance of successively increasing coefficients in $f(x)$, the terms rapidly converge because $x = n_q/n \sim k_B T/E_F \sim 0.01$]. Combining this with the earlier $jE\tau_\epsilon \approx \Delta(T')n_q(T')$, $\eta = j\Phi_0/v = j\Phi_0 B/E$, $\eta \approx H_{c2}\Phi_0/\rho_n$, and $\eta \propto \Delta$, we get a convenient closed form for the nonlinear $j(E)$ characteristic:

$$j \approx \left(\frac{H_{c2}(T_0)}{B\rho_n(T_0)} \right) E\sqrt{f(x)}, \qquad (5)$$

with $x = n_q/n = 0.0245 \times E^2/E^{*2}$, and $E^* = \sqrt{0.0245\rho_n(T_0)Bn\Delta_0/\tau_\epsilon H_{c2}(T_0)}$ is the value of E at the instability peak. We now turn to the experimental details and results.

The samples are c-axis oriented epitaxial films of Y$_1$Ba$_2$Cu$_3$O$_{7-\delta}$ on (100) LaAlO$_3$ substrates with T_c's around 90 K and of thickness $t \approx 90$ nm. Electron-beam lithography was used to pattern bridges of widths $w \approx 2$–20 μm and lengths $l \approx 30$–200 μm. Altogether, ten samples were studied at 12 temperatures (1.6, 2.2, 6, 7, 8, 10, 20, 27, 35, 42, 50, and 80 K) and at 13 flux densities (0.1, 0.2, 0.5, 1, 1.5, 2, 10, 11, 13, 13.5, 13.8, 14, and 15.8 T). The electrical transport measurements were made with a pulsed constant current source, preamplifier circuitry, and a digital storage oscilloscope. The pulse durations t range 0.1–3 μs with ~ 100 ns rise times and ~ 1 ppm duty cycles, resulting in thermal resistances of order 1 nK $\cdot$ cm^3/W. The short thermal diffusion distance ($\sqrt{Dt} \sim 0.001$ cm) allows negligible heat exchange through the leads, and the results were independent of t and the sample environment (vacuum or helium vapor or liquid). The principle of minimum dissipation ensures uniform current flow at high power densities and avoids hot spots, as was verified previously. Further details about the experimental techniques are given in a review article [19]. Note that the j values in the experiment are an order of magnitude lower than the depairing current density [20] and the applied flux densities exceed the self-field of the current by at least 2 orders of magnitude.

Figure 2(a) shows a typical set of experimental $j(E)$ curves. The last stable data point (j^*, E^*) of each curve is at the tail of each arrow. The slightest further increase of $j > j^*$ causes a drastic vertical jump in E as shown by the arrows (the voltage pulse jumps off the scale of the oscilloscope up to the compliance limit of the current source). The jumps show only a small hysteresis $<3\%$ of j^*. (As expected for a current-biased measurement, the break occurs slightly before the slope has become quite vertical [11].) Figure 2(b) shows the same data plotted as the right-hand side of Eq. (5) vs $j - j_{c0}$, the excess current density over the depinning value. The data scale well and tend toward homogeneous linearity. Note that the col-
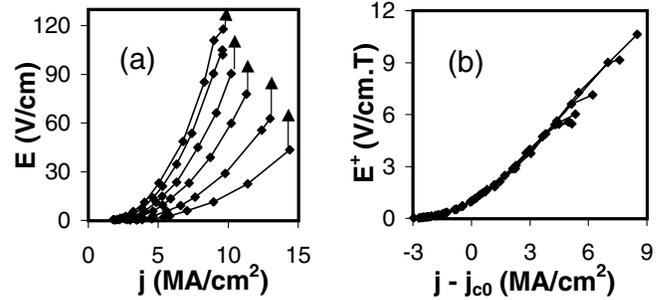

FIG. 2.   Experimental current-voltage characteristics. (a) Raw values of E versus j at $T = 20$ K and applied B values of (from lowest to highest curve) 3, 5, 8, 11, 13.8, and 15.8 T. The last symbol on each curve is right at the instability. Slightest further increase of j (entering the forbidden negative-sloped portion of the theoretical curves of Fig. 1) causes E to make discontinuous vertical jumps (arrows). (b) The same data plotted as $E^+ = (E/B) \times \sqrt{f(0.0245E^2/E^{*2})}$ [as per Eq. (5)] versus $j - j_{c0}$, where the critical depinning current density j_{c0} is defined at $E^+ = 1$ V/cm $\cdot$ T (the scaling is not affected by the choice of criterion).

lapse implies an excellent proportionality between ρ and B over the entire range.

Figure 3 shows experimentally measured B dependencies of v^* and ρ^* for $T_0 = 1.6$ K, demonstrating excellent agreement with Eq. (3) (the other dependencies $E^* \propto \sqrt{B}$ and $j^* \propto 1/\sqrt{B}$ follow from $\rho^* \propto B$ and $v^* \propto 1/\sqrt{B}$). The $v^* \propto 1/\sqrt{B}$ dependence was found to be ubiquitous for all of our low-T measurements in ten samples (spanning 1.6 K $\leq T \leq$ 50 K and 0.5 T $\leq B \leq$ 15.8 T) and has also been seen by Xiao et al. [9] at intermediate temperatures (at the lower end of their $T \sim$ 60–90 K range of study). Note that the excellent linearity between ρ^* and B demonstrates the independence of η on B in this regime; then the resistivity is simply proportional to the number of vortices and hence B.

The final step in the analysis is to extract τ_ϵ from the data. Inverting Eq. (4) evaluated at the instability (i.e., at $T' = T^*$), we get $\tau_\epsilon \approx \frac{\rho_n(T_0)B}{H_{c2}(T^*)E^{*2}} \int_{T_0}^{T^*} c(T)dT$; the $T^*(T_0)$ function comes from the model itself [Fig. 1(b)]. τ_ϵ
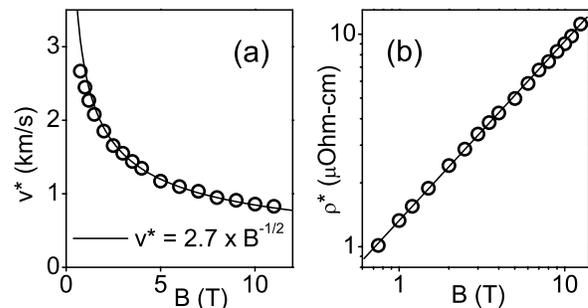

FIG. 3.   Variation of critical parameters with flux density. The measurements were made at $T = 1.6$ K. (a) The critical velocity shows a $v^* \propto 1/\sqrt{B}$ trend (solid line is a $1/\sqrt{B}$ fit). (b) The critical resistivity is proportional to the flux density (straight line is a guide to the eye).
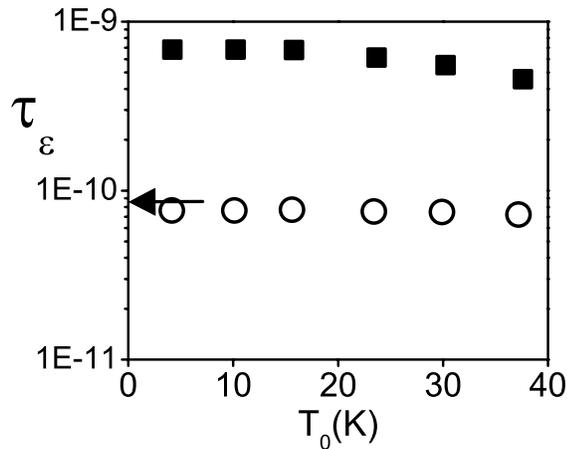
FIG. 4. The energy-relaxation time τ_ϵ extracted from the measured data using the present low-temperature instability model (circles) and from LO theory (squares). The leftward arrow represents the theoretical $T \to 0$ limiting value of $\tau_{e\text{-ph}}$ from phonon emission (please see text).

calculated in this way is shown by the circles in Fig. 4. If the data are analyzed in the LO framework ($\tau_\epsilon \approx D[14\zeta(3)]^{1/2}B^2/(\pi E^{*2})$), a markedly longer τ_ϵ is obtained shown by the squares. For comparison, the arrow shows the theoretical $T \to 0$ limiting value estimated from the spontaneous emission of phonons. [Emission of nonequilibrium phonons dominates e-ph scattering by thermal phonons below a crossover temperature $T_x = m v_F c_s / k_B \approx 43$ K producing an essentially T-independent scattering rate (since $kT \ll E_F$) of $\tau_{e\text{-ph}} = (3\pi \rho_M c_s \hbar^2)/(2C^2 m k_F) \approx 8.4 \times 10^{-11}$, where $C \approx 6 \times 10^{-13}$ ergs is the coupling between electron energy and crystal dilation, $c_s = 4$ km/s is the sound velocity, and $\rho_M = 6$ g/cm^3 is the mass density [21]; see, for example, Kittel [22].]

In conclusion, we investigated the low-temperature regime of flux motion driven far beyond free-flux flow and observed an instability under all conditions of fields and temperatures from $\sim T_c/2$ down to essentially $T \approx 0$. The nature of this low-temperature instability seems to be well described by a model where the electron gas is heated above the phonon temperature, leading to the generation of quasiparticles and loss in viscosity as the vortex core expands and Δ is reduced. This scenario is different from the standard LO picture (dominant mainly near T_c) where the vortex shrinks and quasiparticles leave its vicinity. Because the present effect prevails even at temperatures well below T_c (where most superconductive devices operate), it becomes an important consideration in the design of applications where the superconductor operates in the dissipative regime, since the instability triggers an abrupt rise in dissipation at j values much below the depairing current density. Detailed predictions of the model, including field dependencies of critical parameters and shapes of $j(E)$ curves, were experimentally verified, and

the effect provides an estimate of the $T \to 0$ time scale for energy exchange between quasiparticles and phonons.

*Electronic address: kunchur@sc.edu
http://www.physics.sc.edu/kunchur

[1] A. I. Larkin and Yu. N. Ovchinnikov, in *Nonequilibrium Superconductivity*, edited by D. N. Langenberg and A. I. Larkin (Elsevier, Amsterdam, 1986), Chap. 11.

[2] J. Bardeen and M. J. Stephen, Phys. Rev. **140**, A1197 (1965); M. Tinkham, Phys. Rev. Lett. **13**, 804 (1964); J. R. Clem, Phys. Rev. Lett. **20**, 735 (1968).

[3] N. B. Kopnin and G. E. Volovik, Phys. Rev. Lett. **79**, 1377 (1997).

[4] M. N. Kunchur, D. K. Christen, and J. M. Phillips, Phys. Rev. Lett. **70**, 998 (1993).

[5] A. I. Larkin and Yu. N. Ovchinnikov, Zh. Eksp. Teor. Fiz. **68**, 1915 (1975) [Sov. Phys. JETP **41**, 960 (1976)].

[6] W. Klein, R. P. Huebener, S. Gauss, and J. Parisi, J. Low Temp. Phys. **61**, 413 (1985).

[7] L. E. Musienko, I. M. Dmitrenko, and V. G. Volotskaya, Pis'ma Zh. Eksp. Teor. Fiz. **31**, 603 (1980) [JETP Lett. **31**, 567 (1980)]; A. V. Samoilov *et al.*, Phys. Rev. Lett. **75**, 4118 (1995).

[8] S. G. Doettinger *et al.*, Phys. Rev. Lett. **73**, 1691 (1994).

[9] Z. L. Xiao *et al.*, Phys. Rev. B **53**, 15 265 (1996).

[10] G. M. Eliashberg, JETP Lett. **11**, 114 (1970) [Sov. Phys. JETP **34**, 668 (1972)]; B. I. Ivlev, S. G. Lisitsyn, and G. M. Eliashberg, J. Low Temp. Phys. **10**, 449 (1973).

[11] A. I. Bezuglyj and V. A. Shklovskij, Physica (Amsterdam) **202C**, 234 (1992).

[12] A. I. Bezuglyj, Physica (Amsterdam) **323C**, 122 (1999).

[13] V. G. Voltskaya *et al.*, Sov. J. Low Temp. Phys. **18**, 683 (1993).

[14] S. G. Doettinger *et al.*, Physica (Amsterdam) **251C**, 285 (1995).

[15] H. Nakagawa, N. Miura, and Y. Enomoto, J. Phys. Condens. Matter **10**, 11 571 (1998).

[16] N. R. Werthamer, E. Helfand, and P. C. Hohenberg, Phys. Rev. **147**, 295 (1966).

[17] W. Lanping *et al.*, Phys. Rev. B **40**, 10 954 (1989); R. T. Collins *et al.*, Phys. Rev. Lett. **59**, 704 (1987).

[18] C. Poole, H. A. Farach, and R. J. Creswick, *Superconductivity* (Academic, San Diego, 1995).

[19] M. N. Kunchur, Mod. Phys. Lett. B **9**, 399 (1995).

[20] M. N. Kunchur, D. K. Christen, C. E. Klabunde, and J. M. Phillips, Phys. Rev. Lett. **72**, 752 (1994).

[21] NIST WebHTS Database, http://www.ceramics.nist.gov/srd/hts/htsquery.htm

[22] C. Kittel, *Introduction to Solid State Physics* (Wiley, New York, 1996), 7th ed., appendix J.